Journal of Advanced Ceramics
2013, 2(2): 185–192
DOI: 10.1007/s40145-013-0060-2 ISSN 2226-4108

Research Article

Load-dependent indentation behavior of β-SiAlON and α-silicon carbide

Prasenjit BARICK*, Dulal Chandra JANA, Bhaskar Prasad SAHA

Centre for Non-Oxide Ceramics, *International Advanced Research Centre for Powder Metallurgy and New Materials*, *PO*: *Balapur*, *RCI Road*, *Hyderabad 500005*, *Andhra Pradesh*, *India*

Received: January 23, 2013; Revised: March 31, 2013; Accepted: April 04, 2013

Abstract: A comparative study was carried out on the load-dependent indentation behavior with respect to hardness and induced cracks of β-SiAlON and α-silicon carbide ceramics. It is observed that silicon carbide (SiC) exhibits lower transition load, early cracking and severely crushed indentation sites, whereas β-SiAlON shows higher transition load and damage-free indentation zone even at the maximum applied load (294.19 N). Crack density is higher for α-SiC with comparison to β-SiAlON at each load. SiC exhibits both main and secondary radial types of cracking from low indentation load (0.98 N). Cracks are often associated with branching at higher load (> 9.80 N) for α-SiC. β-SiAlON exhibits cracks which are mainly radial types initiated at 4.90 N load. These opposing behaviors of β-SiAlON and α-SiC are attributed to their difference in hardness, toughness, and brittleness index. Higher brittleness of α-SiC results in early and severe cracking around its indentations. β-SiAlON shows less cracking due to its lower brittleness and higher toughness. The increased size of indentation-induced cracks of α-SiC is higher than that of β-SiAlON due to the rapid crack propagation in α-SiC with transgranular fracture behavior.

Keywords: SiAlON; silicon carbide (SiC); indentation; hardness; crack

1 Introduction

Hardness is the response of a material under specific set of conditions. Hardness of a material depends upon several parameters, including grain size, indenter load and loading rate, indenter geometry, surrounding environment, and accuracy in measurements [1–3]. Generally, hardness decreases with the increase of indenter load and indentation size, known as indentation size effect (ISE) [1,3–8]. This load-dependent hardness phenomenon occurs possibly due to the differential elastic recovery of indentations, cracking and stress relaxation, work hardening, dislocation pinning at the indentation area, and frictional effect between indenter facets and test specimen [1,3].

In general, harder and less tough ceramics, such as boron carbide and silicon carbide, are more brittle than less hard materials with higher fracture toughness, such as zirconia toughened alumina (ZTA) and β-SiAlON.

Previously, extensive research works were carried out on metallic as well as ceramic materials to

* Corresponding author.
E-mail: prasenjit_bhu@rediffmail.com

establish the know-how on load-dependent hardness behavior. The science of ISE was explained by several models, such as Meyer's law, Hays–Kendall approach, elastic recovery model, and proportional specimen resistance (PSR) model [7,9]. Wilantewicz *et al*. [3] have conducted ISE experiment on AlON, AD995 CAP3 Al_2O_3, pressureless-sintered SiC (Hexoloy SA), SiC–N, and SiC–B, using Knoop indenter within the load range of 0.49 N to 137.3 N; it has been shown that for each material, hardness drops by certain percentage (26%, 38%, 36%, 32%, and 31% respectively), and hardness continues to decrease with the increase of load beyond 19.6 N. It has also been shown that crack-dominated indentation area exhibits less hardness than that of less cracked indentation zones for silicon carbide and glasses [3,6]. Quinn and Quinn [10] have shown that beyond transition load, the slope of load–hardness plot becomes asymptotic, and severe crack formation starts beyond this particular load. In another study, the ISE of AlON and $MgAl_2O_4$ spinel was examined concluding that AlON shows rapid decrease in Vickers hardness than that of $MgAl_2O_4$ spinel [11]. Spinel exhibits wider load range (1–3.8 N) before transition load reaches, where deformation rather than fracture is dominant [11].

Silicon carbide (SiC) is a brittle material with hardness of 22–35 GPa and fracture toughness of 2.96–5.8 MPa·$m^{1/2}$ [12,13]; SiC finds applications in the areas of protective system, space mirror, and abrasives [14–16]. β-SiAlON is relatively less brittle than α-SiC, with hardness of 14–17 GPa and fracture toughness of 6.5–7.88 MPa·$m^{1/2}$ [17,18]; β-SiAlON is one of the promising materials for cutting tools, turbine vanes and blades, and turbocharger rotors [19–21]. Hardness has great importance in their applications for both the ceramics. Generally, hardness determines the damage resistance and stiffness of a material; fracture toughness governs the crack propagation behavior of a material under load. Hence, a systematic study was carried out to gain insights about the load-dependent indentation behavior, such as load vs. hardness and indentation-induced cracking of these two ceramics. Since β-SiAlON and α-SiC maintain wide spacing at hardness and toughness scales, it is convincing to consider that the current experimental results can be considered as the reference for other structural ceramics lying within the aforesaid hardness and toughness ranges.

Twelve different loads in the range of 0.49–294.19 N with Vickers indenter were used to carry out the systematic study. The minimum load 0.49 N was chosen, because below this load, indentation size was difficult to measure using inbuilt optical microscope of hardness tester as indentations were smaller in size. The maximum applied indentation load was 294.19 N. This wide load range was chosen because of comparison purpose with respect to cracking behavior between the two ceramics. Beyond 29.4 N load, it was not possible to measure the diagonal size due to severe damage at indentation sites for α-SiC. Hence, load–hardness behavior comparison was made within the load range of 0.49–29.4 N. However, indentations were generated using load upto 294.19 N to show the difference between their indentation-induced cracking characteristics.

2 Experimental procedure

2.1 Materials

The raw premix powders corresponding to β-SiAlON composition were supplied by International Syalons (Newcastle) Limited (United Kingdom) used to produce β-SiAlON ceramics. RTP-SiC powders (D_{50} = 0.8 μm) were supplied by Saint-Gobain Ceramics (Norway) used to fabricate monolithic SiC. β-SiAlON was densified at 1750 ℃ through reaction sintering (liquid phase) of the premix powders, consisting of α-Si_3N_4, AlN, Al_2O_3 and Y_2O_3. Dense α-SiC ceramic was made by solid-state sintering of SiC powders at 2150 ℃. Physical and mechanical characteristics of the sintered products are shown in Table 1. Figures 1 and 2 show the scanning electron micrographs (SEM) of β-SiAlON and α-SiC, respectively.

Table 1 Physical and mechanical properties of β-SiAlON and α-SiC ceramics

	Property	β-SiAlON	α-SiC
Physical	Bulk density (g/cm^3)	3.27	3.16
	Relative density (%)	98–99	98–99
	Apparent porosoty (%)	0.16	—
	Water absorption (%)	0.05	—
Mechanical	$HV_{0.3}$ (kg/mm^2)	1646.00±150.14	2729.00±133.59
	Fracture toughness (MPa·$m^{1/2}$)	8.22±0.66	3.20±0.14
	3 point bend strength (MPa)	700±160	800±25

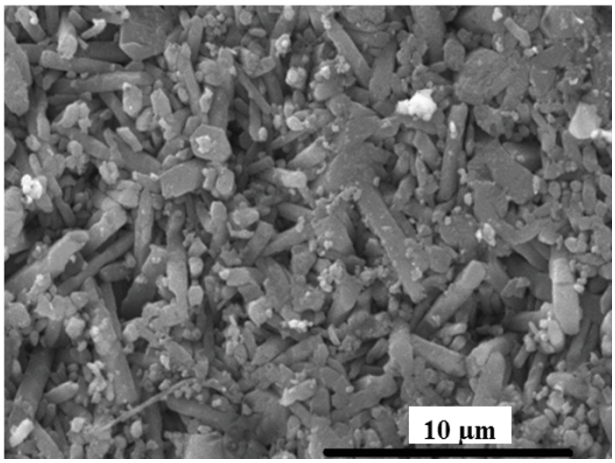

Fig. 1 SEM image for β-SiAlON.

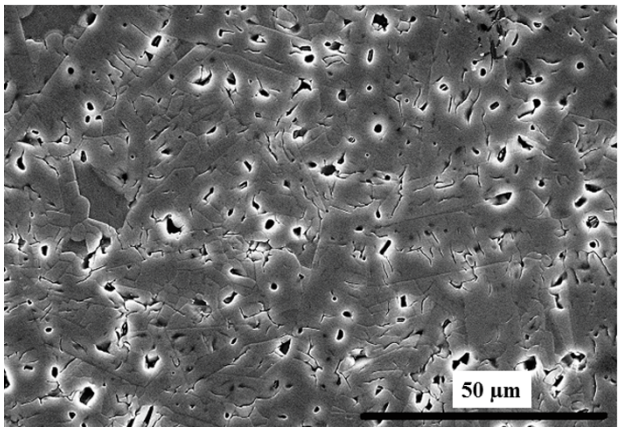

Fig. 2 SEM image for α-SiC.

respectively. β-SiAlON exhibits elongated grains; α-SiC shows equiaxed grains.

2.2 Test specimen preparation

The samples were sectioned from 50 mm × 50 mm × 6 mm sintered blocks using high-speed precision cutting machine (ISOMET 4000, Buehler Ltd., USA). Then samples were hot mounted on a bakelite platform at 100 kg/cm^2 pressure and 120 ℃ temperature using hydraulically operated mounting press (BAINMOUNT, Chennai Metco, India). The sectioned specimens were polished with diamond slurry using variable-speed grinder–polisher (EcoMet 4000, Buehler Ltd., USA). First, the sample was made into maximum flatness using 30 μm diamond gritted disk. Subsequently, polishing was carried out using diamond slurry with the grit-size sequences, e.g., 15 μm, 9 μm, 6 μm, 3 μm and 1 μm, respectively, in descending order.

2.3 Hardness testing

Microhardness tester equipped with Vickers indenter was used for making indentations. This hardness tester (UHL VMHT, Wateruhl Technische Mikroscopie GmbH & Co. KG, Germany) was used to measure microhardness within the load range of 0.49 N to 19.6 N using indenter speed of 50 μm/s with dwell time of 15 s. Further, macrohardness tester (Leco LV 700AT, USA) was used to generate indentations within the load range of 29.41 N to 294.19 N with indentation speed of 50 μm/s and dwell time of 15 s. At each load, 10 best indentations were chosen to generate average hardness data. Linear regression method was applied for best fitting of the hardness data in load–hardness plot. The transition load was determined from their intersecting point. Diagonal lengths of the indentations were measured using inbuilt optical microscope system of hardness tester. Great care was taken during diagonal length measurement in order to minimize the error to a least possible value. The following equation was used to calculate Vickers hardness according to ASTM C 1327:

$$HV = 1.8544(P/d^2)$$

where HV is Vickers hardness (kg/mm^2); P is the indentation load (kgf); d is the average length of the two diagonals of the indentation (mm). Indentation-induced crack propagation behavior and indentation imprints were examined using image analysis software (ANALYSIS 5, Olympus, USA).

3 Results

3.1 Load vs. hardness, indentation size

Figures 3 and 4 show the variation of hardness as a function of indentation load for β-SiAlON and α-SiC, respectively. For β-SiAlON, hardness reduced by 15.47% within the load range of 0.49 N to 29.41 N; α-SiC exhibits reduction in hardness by 31.57% within the identical load range. Hardness data are best fitted by linear regression method, which provides transition load 6.60 N with corresponding hardness of 1511.89 kg/mm^2 for β-SiAlON; α-SiC exhibits transition load 5.67 N with corresponding hardness of 2499.09 kg/mm^2. SiC exhibits brittleness value (B) of 1110.66 μm^{-1}, much higher than that of β-SiAlON (64.44 μm^{-1}). Brittleness parameter was determined using the formula

$$B = H_c E / K_{IC}^2$$

where E is the elastic modulus (GPa); H_c is the critical hardness (GPa); K_{IC} is the fracture toughness (MPa·m$^{1/2}$); B is the ratio of work of deformation to the fracture energy (μm^{-1}) [10]. β-SiAlON exhibits wider load range (i.e., 0.49–6.60 N) than that of α-SiC before transition load appears.

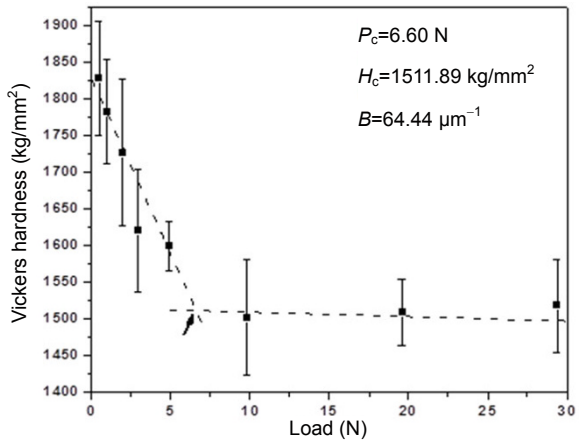

Fig. 3 Load vs. hardness for β-SiAlON.

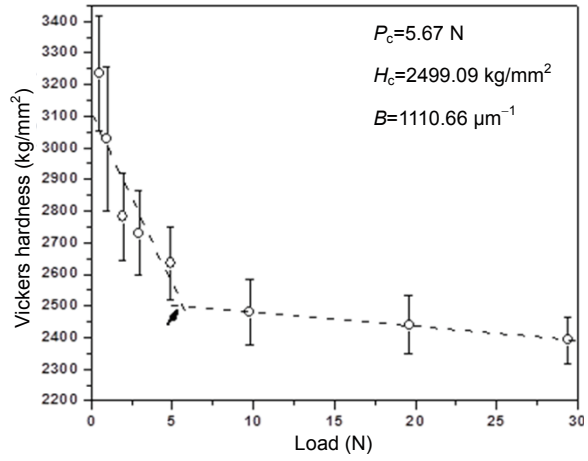

Fig. 4 Load vs. hardness for α-SiC.

Figure 5 shows the variation of indentation size as a function of indentation load for β-SiAlON and α-SiC. Within the said load range, the indentation size increases by 740% and 835% for β-SiAlON and α-SiC, respectively. At each load, the indentation size of β-SiAlON is relatively higher than that of α-SiC as shown in the figure.

3.2 Indentation-induced cracking

β-SiAlON starts showing crack formation after 4.90 N load, whereas α-SiC exhibits crack initiation at 0.49 N load. Cracks are mainly radial type in nature, and no crushed zone is observed even at 294.19 N load for β-SiAlON, as shown in Figs. 6(a)–6(l). Both main and secondary radial types of cracks are found for α-SiC as shown in Figs. 6(m)–6(x). The details of indentation-induced cracks, such as average number of cracks per indentation, minimum and maximum crack sizes at each load, and types of indentation induced cracks, are provided in Table 2. It is observed from Table 2 that the average number of indentation induced cracks per indentation, and crack size are higher for α-SiC than those of β-SiAlON. As the indentation load increases, the crack length also increases significantly.

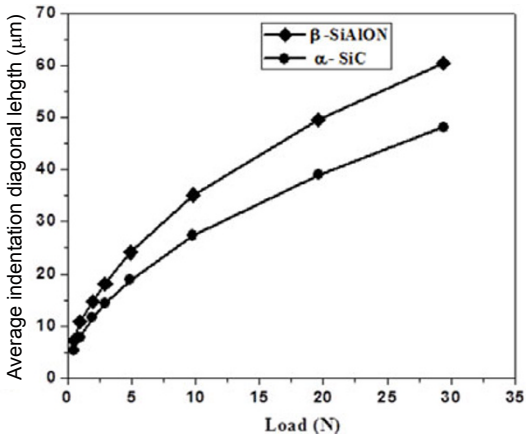

Fig. 5 Load vs. diagonal length of indentations for β-SiAlON and α-SiC.

4 Discussions

In the current study, both materials are demonstrating ISE, i.e., hardness decreases with the increase of load. Among several existing models, elastic–plastic deformation (EPD) is chosen to analyse the ISE phenomena of α-SiC and β-SiAlON, because EPD is a proven technique to explain the ISE of hard and strong materials [22,23]. According to this model, the important origin of ISE in hard and strong materials is that the deformation under the indenter occurs in discrete bands rather than being continuous. Upon removal of load, the recovery of elastic increment of deformation, which precedes each new band of plastic deformation, results in the indentations appearing smaller than expected, particularly at small indentation sizes [22,23]. Thus, the hardness calculated from these residual indentation imprints increases with decreasing contact size, as well as with decreasing load. In the extreme case before the first plastic band is nucleated,

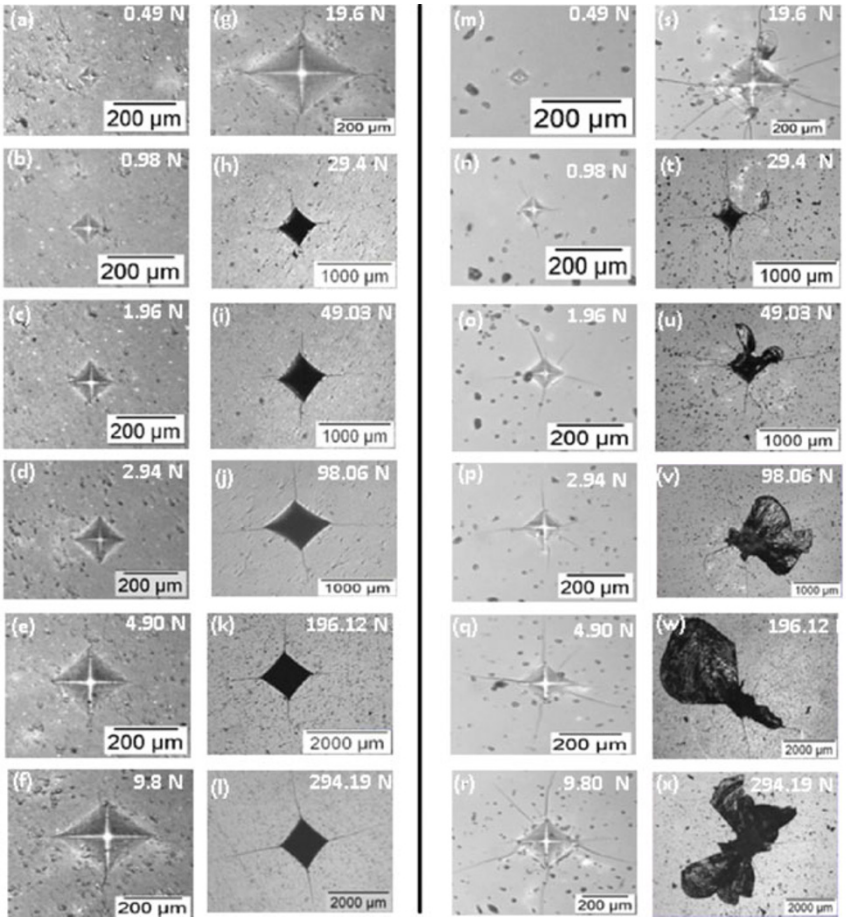

Fig. 6 (a)–(l) Indentation imprints of β-SiAlON at different loads; (m)–(x) indentation imprints of α-SiC at different loads.

Table 2 Number of indention-induced cracks, sizes and types

SI. No.	Load (N)	Average number of cracks per indentation		Minimum crack size (μm)		Maximum crack size (μm)		Type of crack	
		β-SiAlON	α-SiC	β-SiAlON	α-SiC	β-SiAlON	α-SiC	β-SiAlON	α-SiC
1	0.49	X1	2.00	X1	11.94	X1	29.06	X1	Secondary radial
2	0.98	X1	4.00	X1	16.89	X1	55.15	X1	Main radial and secondary radial
3	1.96	X1	4.75	X1	39.00	X1	122.02	X1	Main radial and secondary radial
4	2.94	X1	6.66	X1	36.38	X1	150.06	X1	Main radial with branching and secondary radial
5	4.90	2.00	7.00	4.50	45.95	35.17	218.43	Main radial	Main radial and secondary radial
6	9.80	2.66	9.00	10.13	40.29	65.87	361.88	Main radial	Main radial with branching, secondary radial and crushed zone
7	19.61	4.00	10.00	57.43	244.93	162.16	481.28	Main radial	Crack branching associated with main and secondry radial types; crushed zone is observed
8	29.41	4.00	6.8+partial crushed zone	92.90	271.75	269.37	538.75	Main radial	Crack branching associated with main and secondry radial types; crushed zone is observed
9	49.03	4.00	X2	231.18	X2	423.64	X2	Main radial	Main and secondary radial, associated with severe crushed zone
10	98.06	4.00	X2	334.92	X2	794.33	X2	Main radial	Cracks associated with severe crushed zone
11	196.12	4.25	X2	481.71	X2	1234.41	X2	Main radial and secondary radial	Cracks associated with severe crushed zone
12	294.19	5.00	X2	1018.74	X2	2327.28	X2	Main radial and secondary radial	Severe crushed zone associated with cracks

X1: not exist; X2: crack lengths were not possible to measure because of severe crushed zone.

surface flexure will remain elastic, and fully recoverable on unloading, leaving no residual impression with which to calculate a conventional hardness value [22,23]. At higher load (generally beyond transition), indentations are associated with both elastic deformation and cracking. Fracture and cracking dominate as load increases. Thus, the recovery effect of elastic deformation becomes

negligible, which eventually makes P/d^2 ratios closer at each load. Thus, load–hardness plateau becomes asymptotic particularly at higher load range. The ISE effect in α-SiC is more pronounced than that for β-SiAlON. This behavior of α-SiC and β-SiAlON is further supported by their brittleness parameter, which is much higher for α-SiC (1110.66 μm^{-1}) compared to that of β-SiAlON (64.44 μm^{-1}). The higher brittleness index of α-SiC compared to β-SiAlON, is attributed to its higher hardness at transition load and much lower fracture toughness. The higher percentages of hardness reduction can be interpreted by severe fracture, cracking of SiC combined with its higher percentage indentation size increment.

Due to less hardness and less brittleness of β-SiAlON, it deforms more than α-SiC under the application of load. Therefore, the measured indentation sizes of β-SiAlON remain higher than that of α-SiC at each load within the experimental load range. The difference between indentation sizes of β-SiAlON and α-SiC, gradually increases with load increment, as deformation is more pronounced than fracture for β-SiAlON, whereas fracture dominates over deformation for α-SiC. Since deformation leads higher indentation size than fracture, β-SiAlON exhibits relatively higher indentation size than α-SiC. Because of the similar reason, recovery effect of the incremental part of elastic deformation may persist even at higher load for β-SiAlON, but this effect is expected to be trivial for α-SiC at higher load range as is evident from severe fracture associated with its indentations. Thus, α-SiC demonstrates higher percentages of indentation size increment compared to that of β-SiAlON.

From the indentation imprints (Fig. 6), it is evident that fracture effect at each indentation load is dominant in α-SiC with comparison to β-SiAlON. Because of higher fracture toughness and less hardness, β-SiAlON withstands higher indentation load without damage around indentations due to more deformation effect; SiC is very prone to crack initiation even at low load (0.49 N) due to low fracture toughness and higher brittleness, and exhibits fragmented and irregular-shaped indentations at higher loads. The significant difference in the brittleness parameters of α-SiC and β-SiAlON agrees with the observed damage such as severe cracking and fragmented zone around the indentations of α-SiC. Further, the propensity of crack formation at lower load and development of fragmented indentation zones for α-SiC, are related to its extremely high brittleness; this is also the cause for the formation of different types of cracks namely main and secondary radial types in association with crack branching. On the other hand, due to less brittleness of β-SiAlON, mainly radial cracks appear upon application of indentation load. A higher number of cracks is associated with each indentation for α-SiC than that of β-SiAlON, which is also attributed to higher hardness, higher brittleness and less fracture toughness of α-SiC. Due to high brittleness and transgranular fracture behavior (Fig. 7), crack propagation is much more rapid for α-SiC with comparison to β-SiAlON, which exhibits wavy fracture surface (Fig. 8). This type of fracture surface, which is observed in β-SiAlON, is the indication of relatively more deformation, which prevents rapid crack propagation and reduce indentation-induced crack length. This is the cause for larger-size indentation-induced cracks for α-SiC with comparison to β-SiAlON.

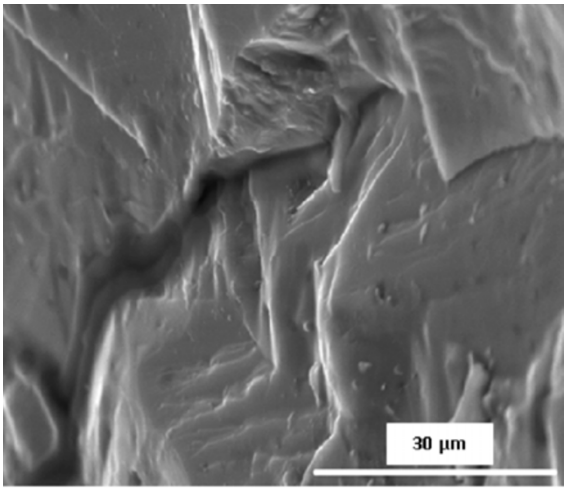

Fig. 7 Fractograph of α-SiC.

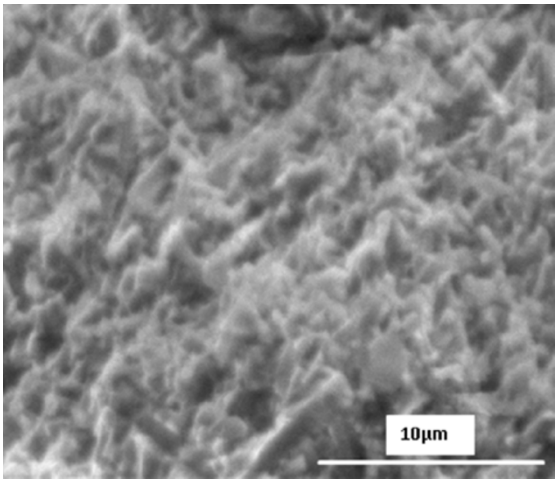

Fig. 8 Fractograph of β-SiAlON.

5 Conclusions

Based on the experimental results, it can be summarized that:

(i) ISE of both structural ceramics is explained by EPD model. Here, ISE is more pronounced for α-SiC than β-SiAlON, as dropping of hardness as a function of load is higher for α-SiC (31.57%) compared to β-SiAlON (15.47%). This effect is due to severe fracture and cracking around indentations combined with higher percentage indentation size increment for α-SiC.

(ii) The combined effect of higher hardness, lower fracture toughness and higher brittleness index is responsible for low transition load, severe cracking and fragmented zones around indentations for α-SiC, whereas effects of lower hardness, higher fracture toughness, and less brittleness make less cracking and crushed free indentations for β-SiAlON.

(iii) Main and secondary radial crack branchings are observed for α-SiC, whereas β-SiAlON exhibits mainly radial cracks. Crack branching is not evident for β-SiAlON. This effect is the cause of extreme brittleness of α-SiC with comparison to β-SiAlON.

(iv) Crack density around indentations is higher for α-SiC than that of β-SiAlON, which is also due to higher brittleness of α-SiC and its less fracture toughness.

(v) Crack sizes at each load are larger for α-SiC than that of β-SiAlON. This is due to the rapid crack propagation in α-SiC because of its transgranular fracture behavior. On the other hand, wavy fracture surface of β-SiAlON is the indication of relatively more deformation, which prevents rapid crack propagation and reduces indentation-induced crack lengths.

Acknowledgements

Authors wish to acknowledge Dr. G. Sundararajan, Director-ARCI, and Dr. Shrikant V. Joshi, Associate Director-ARCI, for their constant inspiration towards the completion of this work.

References

[1] McColm IJ. *Ceramic Hardness*. New York: Plenum Press, 1990.

[2] Rice RW, Wu CC, Boichelt F. Hardness-grain-size relations in ceramics. *J Am Ceram Soc* 1994, **77**: 2539–2553.

[3] Wilantewicz T, Cannon WR, Quinn G. The indentation size effect (ISE) for Knoop hardness in five ceramic materials. In *Advances in Ceramic Armor II*: *A Collection of Papers Presented at the 30th International Conference on Advanced Ceramics and Composites*. Franks LP, Wereszczak A, Lara-Curzio E, Eds. Hoboken: John Wiley & Sons, 2006: 237–250.

[4] Gong JH, Li Y. An energy-balance analysis for the size effect in low-load hardness testing. *J Mater Sci* 2000, **35**: 209–213.

[5] Dusza J, Steen M. Microhardness load size effect in individual grains of a gas pressure sintered silicon nitride. *J Am Ceram Soc* 1998, **81**: 3022–3024.

[6] Quinn GD, Green P, Xu K. Cracking and the indentation size effect for Knoop hardness of glasses. *J Am Ceram Soc* 2003, **86**: 441–448.

[7] Peng ZJ, Gong JH, Miao HZ. On the description of indentation size effect in hardness testing for ceramics: Analysis of the nanoindentation data. *J Eur Ceram Soc* 2004, **24**: 2193–2201.

[8] Sangwal K. Review: Indentation size effect, indentation cracks and microhardness measurement of brittle crystalline solids—Some basic concepts and trends. *Crys Res Technol* 2009, **44**: 1019–1037.

[9] Li H, Bradt RC. The indentation load/size effect and the measurement of the hardness of vitreous silica. *J Non-Cryst Solids* 1992, **146**: 197–212.

[10] Quinn JB, Quinn GD. Indentation brittleness of ceramics: A fresh approach. *J Mater Sci* 1997, **32**: 4331–4346.

[11] Patel PJ, Swab JJ, Staley M, *et al.* Indentation size effect (ISE) of transparent AlON and $MgAl_2O_4$. Available at http://www.arl.army.mil/arlreports/2006/ARL-TR-3852.pdf.

[12] Huang ZH, Jia DC, Zhou Y, *et al*. Effect of a new additive on mechanical properties of hot-pressed silicon carbide ceramics. *Mater Res Bull* 2002, **37**: 933–940.

[13] Zhang XF, Yang Q, De Jonghe LC. Microstructure development in hot-pressed silicon carbide: Effects of aluminum, boron, and carbon additives. *Acta Mater* 2003, **51**: 3849–3860.

[14] Karandikar PG, Evans G, Wong S, *et al*. A review of ceramics for armor applications. In *Advances in Ceramic Armor IV*: *Ceramic Engineering and Science Proceedings*. Franks LP, Obji T, Wereszczak A, Eds. Hoboken: John Wiley & Sons, 2008: 163–175.

[15] Suyama S, Kameda T, Itoh Y. Development of high-strength reaction-sintered silicon carbide. *Diam Relat Mater* 2003, **12**: 1201–1204.

[16] Fernández JM, Muñoz A, de Arellano López AR, *et al*. Microstructure–mechanical properties correlation in siliconized silicon carbide ceramics. *Acta Mater* 2003, **51**: 3259–3275.

[17] Ghosh G, Vaynman S, Fine ME, *et al*. Microstructure and ambient properties of a SiAlON composite prepared by hot pressing and reactive sintering of β-Si_3N_4 coated with Al_2O_3. *J Mater Res* 1999, **14**: 881–890.

[18] da Silva CRM, de Melo FCL, de Macedo Silva OM. Mechanical properties of SiAlON. *Mat Sci Eng A* 1996, **209**: 175–179.

[19] Abo-Naf SM, Dulias U, Schneider J, *et al.* Mechanical and tribological properties of Nd- and Yb-SiAlON composites sintered by hot isostatic pressing. *J Mater Process Tech* 2007, **183**: 264–272.

[20] Hou X-M, Chou K-C, Li F-S. Some new perspectives on oxidation kinetics of SiAlON materials. *J Eur Ceram Soc* 2008, **28**: 1243–1249.

[21] Lin MT, Shi JL, Jiang DY, *et al*. High temperature creep of a hot-pressed β-SiAlON. *Mat Sci Eng A* 2001, **300**: 61–67.

[22] Bull SJ, Page TF, Yoffe EH. An explanation of the indentation size effect in ceramics. *Phil Mag Lett* 1989, **59**: 281–288.

[23] Mukhopadhyay NK, Paufler P. Micro- and nanoindentation techniques for mechanical characterisation of materials. *Int Mater Rev* 2006, **51**: 209–245.